Mechanics & Industry **21**, 408 (2020)
© AFM, EDP Sciences 2020
https://doi.org/10.1051/meca/2020038

Mechanics & Industry

Available online at:
www.mechanics-industry.org

Regular Article

Experimental comparison of the seizure loads of gray iron journal bearing and aluminum alloy journal bearing under aligned and misaligned conditions

Xiuli Zhang[1,*], Zhongwei Yin[2], Qin Dong[2], and Jun Cao[3]

[1] Shandong Provincial Key Laboratory of Precision Manufacturing and Non-traditional Machining, Shandong University of Technology, Zibo, PR China
[2] State Key Laboratory of Mechanical Systems and Vibration, Shanghai Jiao Tong University, Shanghai, PR China
[3] School of Mechanical Engineering and Mechanics, Ningbo University, Ningbo, PR China

Received: 21 March 2020 / Accepted: 5 May 2020

Abstract. Materials, surface roughness of bearing and shaft, and journal misalignment affect the seizure load of journal bearing. To improve the load carrying capacity of bearing and obtain better friction pair, this paper studies experimentally the seizure loads of a gray iron journal bearing and two kinds of aluminum alloy journal bearings under both aligned and misaligned conditions. Three shafts are used to study the effects of journal surface roughness and DLC coating. The journal center locus is recorded. Results show that the combination of DLC coating and the aluminum alloy with lower hardness has the largest seizure load and inclined angle, followed by the combinations of DLC coating and gray iron, and 40Cr steel and gray iron. The surface roughness values of bearing and shaft have a considerable negative effect on seizure load, especially for aligned condition.

Keywords: Journal bearing / Misalignment / Seizure load / Gray iron / Aluminum alloy

1 Introduction

Journal bearings are widely used in rotary compressors. The tribological performance of journal bearing directly affects the operating performance and service life of compressor. With the development of compressors with high efficiency, high reliability, low noise, low cost and compact structure, the demand for journal bearings with larger load carrying capacity, larger permissible misaligned angle and lower friction coefficient is growing. The lubrication and load carrying performances of journal bearing are affected by structural parameters, rotational speed, lubricants, materials of bearing and shaft, surface roughness of bearing and shaft, journal misalignment and so on. By studying the influence of these parameters on bearing load carrying capacity, we can provide guidance for the design of journal bearings in rotary compressors. The effects of bearing clearance, length-to-diameter ratio, diameter, rotational speed and surface roughness of bearing and shaft on the load carrying capacity of misaligned bearings have been studied in our previous work [1,2]. In this work, we focus on the effect of bushing and shaft material on the load carrying capacity of journal bearing under aligned and misaligned conditions. The effects surface roughness of journal and shaft are also analysed.

Gray iron and aluminum alloys are the most widely used bushing materials in compressor due to the low-cost and good performance. Many researches have studied their tribological properties. Biswas and Rohatgi [3] compared the tribological properties of two graphitic aluminium composites, the aluminium alloy on which they were based and commercial-quality bronze, and found that the graphite-aluminium composites perform the best. Desaki et al. [4] developed a new aluminum alloy bearing with higher resistance and found that the mechanism of the wear resistance improvement is that the load is resisted by the concentrated Si on the sliding surface that is held strongly by sufficient hardness of the matrix. Feyzullahoglu and Sakiroglu [5] studied the friction and wear properties of four different aluminum alloys on pin on disc wear tester and found that Al-Sn and Al-Si alloys have better wear properties than Al-Pb alloys. Prasad [6] investigated the influence of applied load, sliding speed and test environment on the sliding wear behaviour of a gray iron by pin-on-disc tests. Summer et al. [7] carried out tribological testes with a ring-on-disk test configuration studying the performance of forged steel and cast iron sliding against

* e-mail: zhangxiulli@163.com

an Al based bearing alloy under start-stop operation. Results showed that the performance of forged steel depends on the overall roughness of the surface, whereas the tribological functionality of cast iron is mainly determined through its microstructure and the occurrence of metal flaps with burrs. Most of the research on the tribological properties of bushing materials used the pin-on-disc test rig and did not consider the effect of misalignment. The results generally showed the friction coefficient and wear rate (depth) of the material, and cannot tell the ultimate load carrying capacity of journal bearing with the material.

Surface roughness values of shaft and bearing affect the film thickness distribution, and thus affect the lubrication performance. Many researchers studied the effect of surface roughness on bearing performance. For example, Guha [8] analysed the steady state characteristics of misaligned hydrodynamic journal bearings with isotropic roughness effect and found that the load capacity decreases with an increase in the roughness parameter. Bujurke et al. [9] investigated the effect of surface roughness on the squeeze film characteristics of long porous partial journal bearings with couple stress fluids as lubricant and found that the transverse (longitudinal) roughness pattern increases (decreases) the load carrying capacity. Sun et al. [10] studied the effect of surface roughness, viscosity-pressure relationship and elastic deformation on lubrication performance of misaligned journal bearings by numerical calculation. It was found that when not considering the deformation, the surface roughness has effects on the bearing lubrication performance for large eccentricity ratios, but have little effect when considering the deformation. However, those literature mainly carried out the researches by numerical method. There is still a dearth of experimental researches on the relation between surface roughness and load carrying capacity of bearing. In our previous work [2], the relation was studied by experiments, but as the radial clearance was only 10.5 μm, the seizure loads for aligned condition reached and exceeded the designed maximum load of the test rig, 4900 N. The effects of shaft deformation and viscosity-temperature limited the increase of bearing seizure load under aligned condition. In this work, the bearing radial clearance is increased to more than 22 μm and the effect of surface roughness on seizure load is evaluated.

The effect of journal misalignment on lubrication performance of journal bearings has been studied by both numerical and experimental methods. Bouyer and Fillon [11] measured the pressure and temperature fields in the mid-plane of the bearing, temperatures in two axial directions, oil flow rate, and minimum film thickness for various operating conditions and misalignment torques. It was found that the bearing performances were greatly affected by the misalignment. The maximum pressure in the mid-plane decreased by 20 percent for the largest misalignment torque while the minimum film thickness was reduced by 80 percent. Pierre et al. [12] developed a thermohydrodynamic (THD) model for misaligned plain journal bearings and studied the influences of misalignment torque and direction on shaft position, pressure field and temperature field. Sun et al. [13,14] studied experimentally and numerically the effect of journal misalignment caused by shaft bending on the lubrication performance of journal bearings and found that the higher the load on the shaft, the larger the journal misalignment, the more obvious effect on lubrication performance of journal bearing. Nikolakopoulos and Papadopoulos [15,16] analysed the friction coefficient of worn misaligned journal bearings and found that the friction coefficient is strongly dependent upon the misalignment angle and the power loss is increased with wear depth. Thomsen and Kilt [17] proposed a flexure journal bearing design and investigated the improvement of bearing performance at heavy misalignment by a thermoelastohydrodynamic (TEHD) model. Mallya et al. [18,19] calculated the steady state characteristics of a misaligned multiple axial groove water-lubricated journal bearing in the laminar regime and in the turbulent regime respectively. Li et al. [20] investigated the influence of dissimilar radial clearances of two end bearings on the performance of hydrodynamic rotor-bearing systems under rotor misalignment effects and found that the inequality should not be neglected. Lv et al. [21] proposed an approach for efficiently analysing equivalent supporting point location and carrying capacity of misaligned journal bearing without using numerical simulation. Li et al. [22] developed a new model considering the axial movement of journal, the surface topography of journal and bearing and the misalignment of journal, and analysed their effects on the lubrication performance of misaligned journal bearing. Zhang et al. [23] carried out a TEHD analysis of misaligned bearings with texture on journal surface under high-speed and heavy-load conditions. Mo et al. [24] studied the lubrication performance of a pre-tilted journal bearing by experiments and fluid-structure (FSI) interaction method, and found that the pre-tilted journal bearing can improve the oil film pressure distribution and the frequency spectrum. Zheng et al. [25] investigated the performance characteristics of misaligned journal bearing lubricated using couple stress fluids by numerical method. Zhu et al. [26] analysed the thermal turbulent lubrication performance of rough surface journal bearing with journal misalignment. While the above researches mainly studied the operating properties such as minimum film thickness, pressure and temperature distribution, friction coefficient, and dynamic characteristics of misaligned journal bearings. There is still little literature about the limit of seizure failure of misaligned journal bearings.

In this work, the seizure loads of a gray iron journal bearing and two kinds of aluminum alloy journal bearings were investigated experimentally for both aligned and misaligned conditions. Two 40Cr shafts with different surface roughness and a shaft with DLC coating were tested with the bearings. The effects of bushing material, shaft coating, and journal surface roughness on seizure load were analyzed. The journal center locus was recorded and the effects of radial clearance and surface roughness on ε-F curve were studied. The changes of journal center displacement and bearing deformation at the edge with misalignment angle were also studied and analyzed.

2 Experimental system

2.1 Test rig

Figure 1 shows the schematic of the journal bearing test rig, and Figure 2 is the photo of the test rig. The main shaft is supported by three rolling bearings and powered by a variable frequency motor through a belt drive. The rotational speed of the shaft was set to 1200 r/min in the seizure tests. The test bearing is mounted in a sleeve with two end covers. Two ball bearings are installed outside the sleeve so that the friction torque can be measured by force sensor 2. The whole test device is pulled by a leading bar. The load is applied using lever principle by rotating the hand wheel and measured by force sensor 1. The misalignment angle of the test bearing is adjusted by a micrometer head and a ball roller. The bearing is flood lubricated by oil. The oil is supplied by a peristaltic pump which can control the flow rate. The oil flow rate is maintained at 50 ml/min for gray iron bearing and 25 ml/min for other bearings. The temperature of oil is controlled at 35 ±1°C by water bath, and the oil viscosity is about 0.01 Pa.s. Table 1 presents the basic information of test bearing and lubricant.

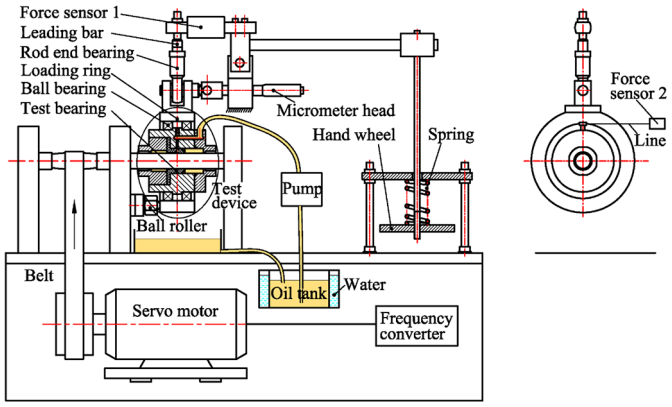

Fig. 1. Schematic of test rig.

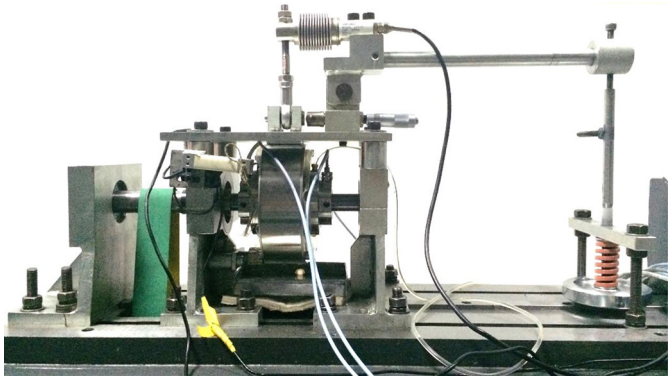

Fig. 2. Photo of test rig.

2.2 Measure of inclined angle and journal center position

Figure 3 shows the arrangement of four sensors. Sensors are installed on the two covers. As the load is exerted on the test bearing and no load is exerted on the two end covers, the sensors on the covers move with the test bearing as load increases. Thus, the distance between sensor and test bearing axis is considered to be constant. Sensors a and c measure the vertical displacement of test bearing relative to journal surface. Sensors b and d measure the horizontal displacement of test bearing relative to journal surface.

Figure 4 presents schematic of the measurement of inclined angle and journal center position regardless of deformation and wear. The red line refers to the axis of shaft. The blue line refers to the axis of bearing. Relative to the bearing axis, there are a bottom position and a top position for the shaft axis. The distance between the bottom (top) position of shaft axis and bearing axis is the radial clearance. $a_i\,(i=1,2...)$ refers to the measurement of sensor a for different conditions. The black circle in left side view (in first angle projection) refers to the clearance circle. The red cross and the blue cross refer to the journal center and bearing center in the mid-plane of the test bearing, respectively. The bearing center is set to the coordinate origin. By recording the measurements of four sensors, the relative displacement between shaft and bearing can be calculated.

Figure 4a shows the condition when the shaft and bearing come into contact in seizure tests, which can be used to calibrate the journal center position. The measurements a_0, b_0, c_0 and d_0 are taken as standard values. In this condition, the shaft axis is on the bottom right of the clearance circle. The x coordinate of journal center, x_0, can be determined approximately by the scratches on the bearing surface (see Fig. 18). For most cases, seizure happens at this condition, and the wear depth of bearing is very small. Then the y coordinate of journal center, y_0, can be calculated by $x_0{}^2 + y_0{}^2 = c^2$, where c is the radial clearance. For other cases, seizure doesn't happen or happens when the bearing has been seriously worn. For these cases, the measurements can reflect the condition when the bearing and shaft come into contact. As seen in Figures 15c and 16a, the x coordinate value increases as the load increases after the bearing and shaft come into contact. Then y_0 can be determined. When the shaft operates under the condition as shown in Figure 4b, coordinates of the journal center in the mid-plane of

Table 1. Basic information of test bearing and lubricant.

Bearing diameter	D (mm)	22
Bearing length	L (mm)	22
Diameter of oil hole	d_h (mm)	2.5
Lubricant type	–	ISO VG 10
Oil density	ρ (kg/m^3)	868
Oil viscosity at 35 ± 1°C	μ (Pa.s)	0.01024 ± 0.00035

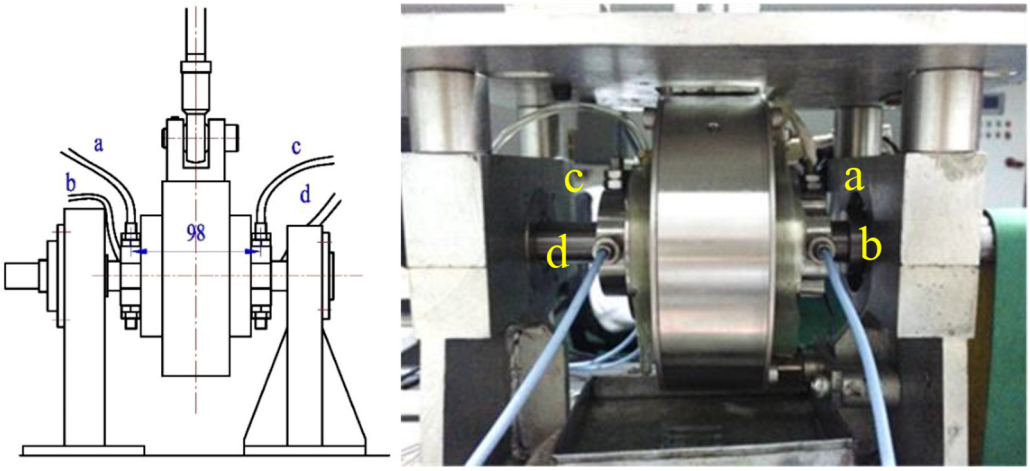

Fig. 3. Arrangement of sensors.

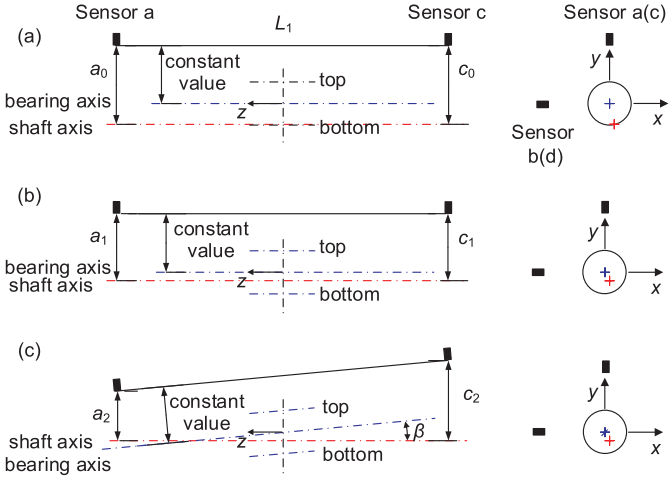

Fig. 4. The position of bearing axis relative to shaft axis regardless of deformation and wear (a) for seizure load under aligned condition, (b) under aligned condition, and (c) under misaligned condition.

bearing will be

$$x = x_0 + \frac{(b_1 + d_1) - (b_0 + d_0)}{2}$$
$$y = y_0 - \frac{(a_1 + c_1) - (a_0 + c_0)}{2}. \quad (1)$$

In the analyses of journal center position, the average measurement of sensors a and c (or sensors b and d) is used to reduce experimental errors.

For the misaligned condition, the vertical inclined angle (β) can be calculated using the following equation.

$$(c_2 - c_1) - (a_2 - a_1) = L_1{}^*\tan\beta \quad (2)$$

where L_1 is the distance between the measured point $a(b)$ and $c(d)$. It is 98 mm.

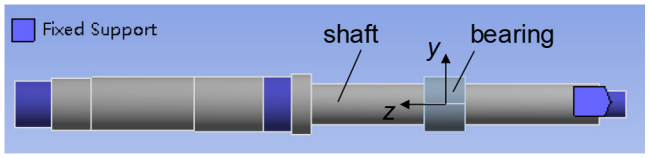

Fig. 5. Calculation model for shaft and bearing deformation.

In the experiments, an unneglected problem is that the shaft will deform under load. The larger the load, the larger the deformation. Shaft deformation affects the measurements of sensors, i.e., the measurements in the bearing lubrication performance test include two parts: one is the variation of journal center position and the other one is the shaft deformation. To evaluate the effect of shaft deformation on measurements, the deformations of shaft and bearing under different loads were calculated by ANSYS static structural analysis. Figure 5 shows the calculation model. The material of shaft is 40Cr steel with $E = 200$ GPa, $\nu = 0.3$, and the material of bearing is gray iron with $E = 110$ GPa, $\nu = 0.28$. The blue journal surfaces are fixed. The load is applied on the lower outer surface of bearing in y direction. Figure 6 presents the deformation and equivalent stress of shaft and bearing for $F = 5000$ N. The maximum equivalent stress is less than the yield stress of material, thus the deformation is elastic. As the sensors move with the bearing, Figure 6a shows that the measurements of sensors a and c increase with the increasing load due to shaft deformation. The average measurement of sensors a and c increases 35.7 μm for $F = 5000$ N in theory. Measurements of sensors b and d also vary with load because the measured points change.

However, due to the internal clearance and installation clearance of the two rolling bearings supporting the shaft, the actual deformation is different from the calculated values. To eliminate the deformation values, a static calibration test needs to be carried out after the seizure test to record the measurement variation of sensor a (b, c, d) because of the shaft deformation under the same load as ai (bi, ci, di). If Δai (Δbi, Δci, Δdi) defines the measurement

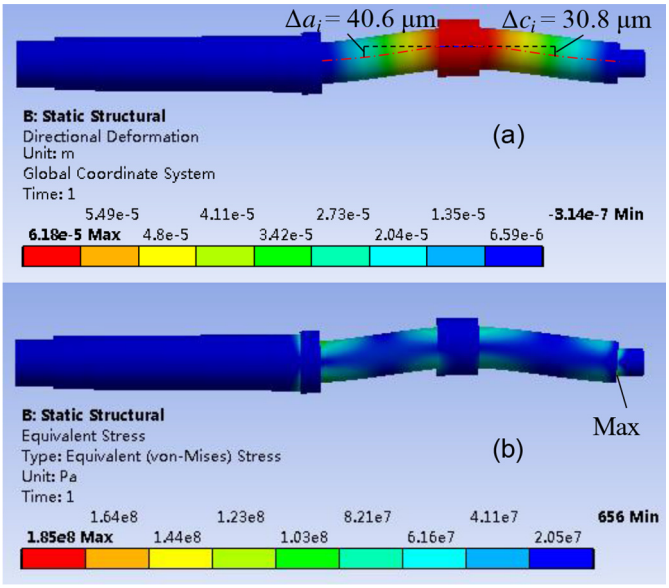

Fig. 6. (a) Deformation, (b) equivalent stress of shaft and bearing for $F = 5000$ N (scale factor: 140).

variations due to the shaft deformation, equation (1) should be revised to the following equation.

$$x = x_0 + \frac{(b_1 + d_1) - (b_0 + d_0)}{2} - \frac{\Delta b_1 + \Delta d_1}{2}$$
$$y = y_0 - \frac{(a_1 + c_1) - (a_0 + c_0)}{2} - \frac{\Delta a_1 + \Delta c_1}{2}. \quad (3)$$

Then, the eccentricity ratio and attitude angle can be given by

$$\varepsilon = \sqrt{x^2 + y^2}$$
$$\phi = \arctan(-x/y). \quad (4)$$

2.3 Determination of seizure load

2.3.1 Seizure load under aligned condition

The determination method of seizure load under aligned condition is similar to that mentioned in previous work [2]. But the seizure process has different characteristics for different bushing materials. For bushings A and B, the friction torque increased sharply when seizure failure happened. Thus, it was much easier to determine the seizure load. For bushing C, as the load increased, the friction torque increased to a larger value, but seizure didn't happen. After a long-time running, the bearing was worn seriously under heavy load, and seizure still didn't happen. This is mainly due to the low friction coefficient and poor wear resistance of the bushing material. As excessive wear should be avoided, the load at which the friction didn't decrease and began to increase was considered as the seizure load of bushing C. The load was increased by 196 N at low load and by 98 N at high load. For each load, the bearing ran for at least 10 min to see if the friction torque was stable.

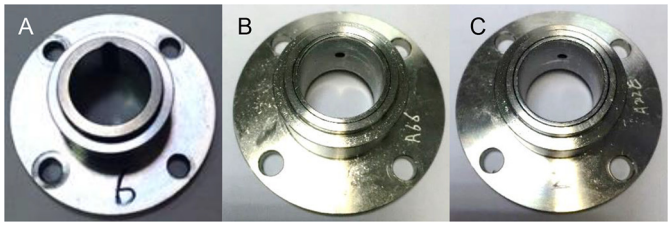

Fig. 7. Test journal bearings with three different bushing materials.

Table 2. Chemical composition (%) of bushings B and C.

	Al	Cu	Sn	Si
Bushing B	87	1	6	6
Bushing C	87	1	12	0

Fig. 8. Photo of aluminum alloy bushings.

2.3.2 Seizure load under misaligned condition

For the misaligned condition, the seizure loads for $\beta = 0.5$ mrad and 1.0 mrad are mainly studied. As the inclined angle is definite, the seizure load value for the inclined angle was estimated and added on the test bearing firstly. Before the test device was inclined, the standard values as shown in Figure 4b was recorded. Then the test device was inclined until the inclined angle was the given value. If the friction torque was stable, the load was increased and the inclined angle was adjusted until seizure failure happened. If the inclined angle could not be increased to the given value, the load was decreased and the inclined angle was adjusted until seizure failure happened when the inclined angle was the given value. For each inclined angle, the seizure test was repeated twice for accuracy.

3 Experimental scheme and test specimens

Figure 7 shows the test journal bearings. The journal bearing is composed of bearing sleeve and bushing. The material of bearing sleeve is 45 steel. Bushing A is made of Grade 250 gray iron. Bushings B and C are two kinds of aluminum alloy with different hardness. Their chemical compositions are shown in Table 2. The gray iron bushing is made from a casting. The aluminum alloy bushings are products of Daido Metal Co., Ltd (see Fig. 8). To improve the seizure load of journal bearing under misaligned condition, a ring groove is machined at one end of the

Table 3. Test journal bearings.

Bearing	Material	D (mm)	$R_{a,b}$ (μm)
A	Grade 250 gray iron	ϕ22.050	0.31–0.36
B	Aluminum alloy 1	ϕ22.048	0.78–1.30
C1	Aluminum alloy 2	ϕ22.048	0.68–0.81
C2	Aluminum alloy 2	ϕ22.047	0.66–0.97

Fig. 9. Test shafts.

Table 4. Test shafts.

Shaft	Material	d (mm)	$R_{a,j}$ (μm)
a	40Cr steel	ϕ21.995	0.09–0.12
b	40Cr steel	ϕ21.998	0.31–0.35
c	DLC coating	ϕ21.996	0.08–0.11

bearing. The bearing thickness is reduced from 7 mm to 3.5 mm at the end, and the depth of the ring groove is 3 mm.

Table 3 shows the measured diameter and surface roughness of the tested bearings. The diameters of bearings are around ϕ22.048 mm. The surface roughness of bearing A is Ra 0.31–0.36 μm. It is measured in the axial direction at six points along the circumference. Due to the material properties and the grinding process, the surface roughness values of aluminum alloy bearings are much larger than that of gray iron bearing. Two bearing C were used in the experiments. It is because during the experiment of bearing C, it was found that due to the low hardness and poor wear resistance of bushing C, the friction increased as load increased but seizure failure didn't happen, then bearing C1 was seriously worn in the initial experiment. Then bearing C2 was used for other experiments, and to avoid wear the load at which the friction didn't decrease and began to increase was considered as its seizure load. For bushings A and B, it was easy to determine when seizure failure happened, thus the bushing wear was negligible and the inner diameters changed little after experiments. So bearings A and B were used repeatedly for the seizure test with different shafts.

Three shafts were tested with the bearings to study the effects of surface roughness and surface coating of shaft on the seizure load of journal bearing. Figure 9 is the photo of the shafts. Table 4 shows the actual parameters of the shafts. The shafts are made of hardened 40Cr steel. The diameters of shafts a–c are ϕ21.995 mm, ϕ21.998 mm and ϕ21.996 mm respectively. The measured surface roughness of the three shafts are Ra0.09–0.12 μm, Ra0.31–0.35 μm, and Ra0.08–0.11 μm respectively. For shaft c, there is a layer of diamond-like carbon (DLC) coating on the surface. DLC coating is a nanocomposite coating that has unique properties of natural diamond such as low friction (0.05–0.2, vs steel, no lubricant), high hardness (>2500 HV), and high wear resistance. The thickness of DLC coating on shaft c is 1.98 μm. For each shaft, the seizure loads of different bearings were investigated for both aligned and misaligned conditions. The radial clearance values of different friction pairs are summarized in Table 5.

4 Results and discussion

4.1 Seizure loads for different bearings and shafts

Table 6 summarizes the seizure loads of different friction pairs for both aligned and misaligned conditions. Figures 10 and 11 present the variation of seizure load with misaligned angle for different friction pairs.

Figure 10 presents that for shafts a and b, the seizure load of the three bearings from high to low in order is A (gray iron), C (aluminum alloy 2), B (aluminum alloy 1) for both aligned and misaligned conditions. Thus, when the shaft material is 40Cr steel, the seizure load of Grade 250 gray iron is the highest, and the seizure load of the aluminum alloy 1 with larger hardness is the lowest under both aligned and misaligned conditions. It illustrates that the friction coefficient of 40Cr steel and aluminum alloy 1 is large and they are not an ideal friction pair.

For shaft c (DLC coating), the seizure load of different bushing materials in decreasing order is C (aluminum alloy 2), A (gray iron), B (aluminum alloy 1). That is, when there is a layer of DLC coating on the shaft surface, the seizure loads of the aluminum alloy with lower hardness and Grade 250 gray iron are the highest, and the seizure load of the aluminum alloy with larger hardness is still the lowest. Figure 11 shows that the seizure loads of bearings A, B and C2 with shaft c are much larger than those with shafts a and b due to the high hardness and low friction coefficient of DLC coating. The seizure loads of bearings A and C2 with shaft c for aligned condition even reach and exceed the designed maximum load of the test rig, 4900 N. The maximum inclined angles also increase. The results demonstrate that the DLC coating helps to improve the seizure load of these bearings under both aligned and misaligned conditions, as well as the maximum inclined angle under certain load.

It is difficult to obtain the same surface roughness for the three kinds of bearing materials. For gray iron, it is easy to get a smaller surface roughness by precise-boring machining. But for others, as the machining allowances of bushing are small, internal grinding was employed and the surface roughness values are larger. Thus, the results are affected synthetically by the material and surface roughness of bearing. In the previous work, it has been found that the smaller the surface roughness of bearing, the larger the seizure load [2]. The results here show that in most cases, the seizure loads of bearing A (gray iron) are larger than those of bearings B and C, and the seizure loads of bearing C are larger than those of bearing B. This is in

Table 5. Radial clearances of different friction pairs.

Bearing	Shaft		
	a (Steel, Ra0.09–0.12)	b (Steel, Ra0.31–0.35)	c (DLC, Ra0.08–0.11)
A (Gray iron, Ra0.31–0.36)	27.5	26	27
B (Aluminum 1, Ra0.78–1.30)	26.5	25	26
C1 (Aluminum 2, Ra0.68–0.81)	26.5	–	–
C2 (Aluminum 2, Ra0.66–0.97)	–	24.5	25.5

Table 6. Seizure loads of different friction pairs for aligned and misaligned conditions Unit: N.

Bearing	Shaft		
	a (Steel, Ra0.09–0.12)	b (Steel, Ra0.31–0.35)	c (DLC, Ra0.08–0.11)
A (Gray iron, Ra0.31–0.36)	0 mrad: 4626 0.5 mrad: 3107, 3361 0.8 mrad: 2068, 1980	0 mrad: 3067, 3165 0.5 mrad: 2293, 2087	0 mrad: >4900 1 mrad: 4900 1.1 mrad: 2960 1.45 mrad: 1539
B (Aluminum 1, Ra0.78–1.30)	0 mrad: 1695, 1872 0.5 mrad: 882, 951	0 mrad: 1499, 1617 0.5 mrad: 960	0 mrad: 3724, 3851 0.5 mrad: 1842, 1980 1 mrad: 1039, 980
C (Aluminum 2, Ra0.66–0.97)	0 mrad: 3626, 3920 0.5 mrad: 1891, 2156 1 mrad: 1019	0 mrad: 1744, 1695 0.5 mrad: 1254, 1205 1 mrad: 647, 598	0 mrad: >4900 1.18 mrad: 4900 1.46 mrad: 2940

consistent with the conclusion in the previous work. To get a deep insight, the effect of bearing surface roughness on ε–F curve is discussed in Section 4.2.

Compared the results of bearings with shaft a and shaft b (see Fig. 11), it can be found that the seizure loads of almost all bearings with shaft b (Ra0.31–0.35) are smaller than those of bearings with shaft a (Ra0.09–0.12). Thus, the larger the journal surface roughness, the smaller the seizure load. The seizure load of bearing A with shaft b is about 32% smaller than the result with shaft a for $\beta = 0$ and 0.5 mrad. The seizure load of bearing B with shaft b is about 13% smaller than that with shaft a for $\beta = 0$, but a bit larger than that with shaft a for $\beta = 0.5$ mrad. The seizure load of bearing C2 with shaft b is about 54% smaller than the result of bearing C1 with shaft a for $\beta = 0$ and about 39% smaller for $\beta = 0.5$ mrad and 1 mrad. It illustrates that the journal surface roughness has a considerable negative effect on seizure load of bearing, especially for aligned condition.

Moreover, it should be noticed that the diameter of shaft a is 3 μm smaller than that of shaft b, that is, the clearance of all bearings with shaft a is 1.5 μm larger than that with shaft b. In theory, the larger the clearance, the smaller the load carrying capacity for aligned condition. However, the seizure loads of all bearings with shaft a are larger than those with shaft b. This indicates that the journal surface roughness has a greater influence on seizure load than the radial clearance here. But as the variation of radial clearance is small, the conclusion has limitations. The effect of clearance on seizure load for both aligned and misaligned conditions were studied in the previous work. As the radial clearance increases from 10.5 μm to 21.5 μm, the seizure load decreases by 51% for aligned condition and increases 1.7 times for $\beta = 0.6$ mrad [2]. The clearance has a significant influence on seizure load for a wider range.

4.2 Journal center locus for different bearings and shafts

Figure 12 presents the variation of average measurements with load in x (sensors b and d) and y (sensors a and c) directions for a seizure test (green line) and the corresponding static calibration test (red line). The blue line is calculated by equation (3) using the red and green datasets. It denotes the variation of journal center coordinate values in the clearance circle. Thus, the variation can be drawn in x-y coordinates as shown in Figures 15–17. The variation of eccentricity ratio and attitude angle can be obtained using equation (4).

Figure 13 shows the variations of eccentricity ratio and attitude angle versus load for the three kinds of bearings with different shafts under aligned condition. It can be seen that the eccentricity ratio increases rapidly to 0.7 when the load increases to 200–400 N, which means that the load carrying capacity of bearing is very low for small eccentricity ratios. When the eccentricity ratio is larger than 0.9, the load carrying capacity increases sharply as the eccentricity ratio increases. Under heavy load, bearings B and C were worn as shown in Figure 18 and the eccentricity ratios for some cases in Figure 13(c, e) exceed 1. The attitude angle is about 60° under low loads. But as the bearing stiffness is small under low load conditions, the initial attitude angles for different friction pairs vary a lot.

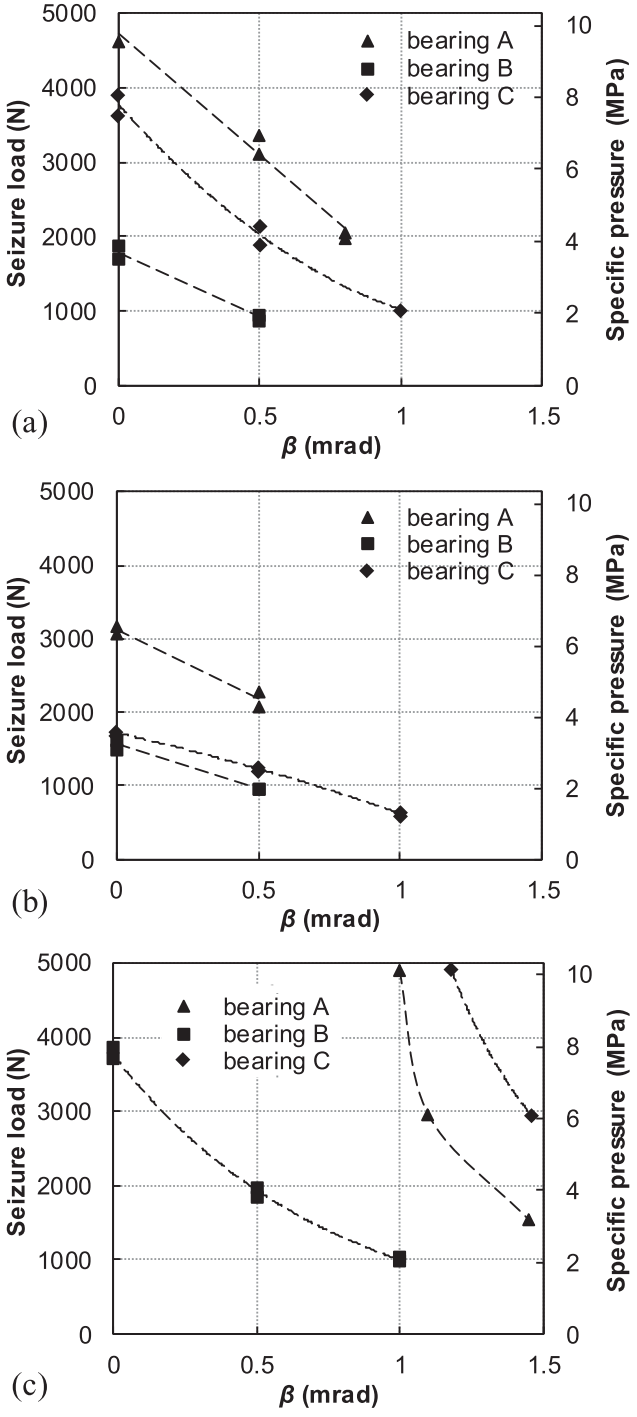

Fig. 10. Seizure loads of three bearings with (a) shaft a, (b) shaft b and (c) shaft c (Specific pressure = F/LD).

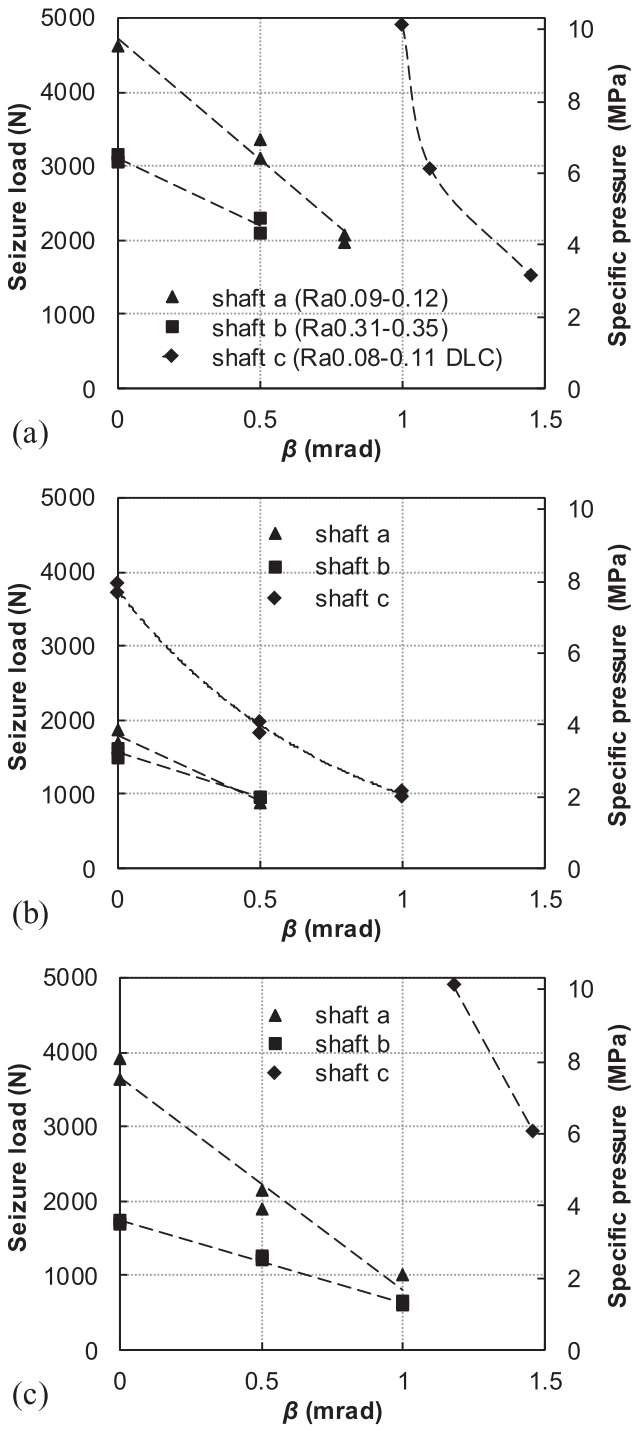

Fig. 11. Seizure loads of (a) bearing A, (b) bearing B and (c) bearing C for different shafts.

As the load increases, the attitude angle finally decreases to 10°–20°, which can also be seen from the wear surfaces of the bearings (see Fig. 18).

The curves of ε–F for different friction pairs are a little different from each other. In Figure 13a, the eccentricity ratio of bearing A with shaft a is much larger than those with shafts b and c for F <3000 N, and the eccentricity ratio of bearing A with shaft c is slightly larger than that with shaft b for F <1300 N. This can be explained by the different clearances. The clearances of bearing A with shafts a, b and c are 27.5 μm, 26 μm and 27 μm, respectively. For the same load, the larger the clearance, the larger the eccentricity ratio. The larger eccentricity ratio of bearing A and shaft a might also be caused by the scratches on the surface of bearing A as shown in Figure 18Aa. Figure 18A0 is the original bearing surface,

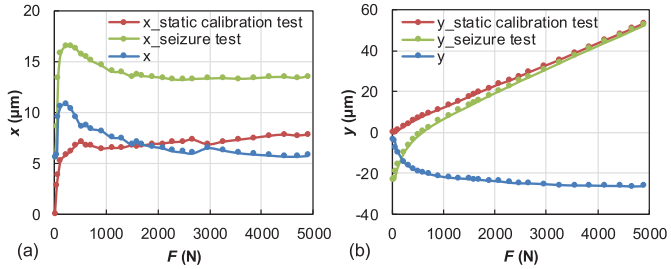

Fig. 12. Variation of average measurements for a seizure test (green line) and the corresponding static calibration test (red line) for bearing A and shaft c. Blue line shows the journal center coordinate values in clearance circle calculated by Equation (3).

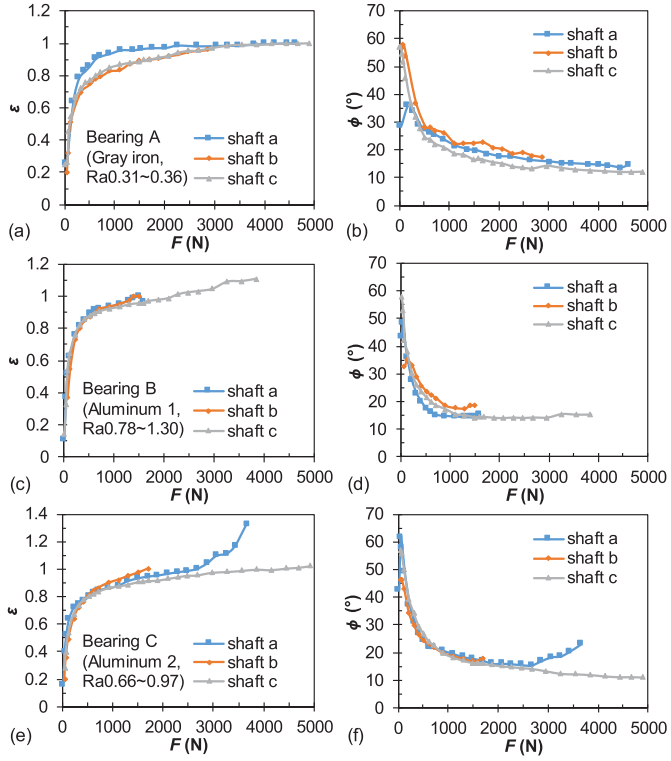

Fig. 13. Eccentricity ratio and attitude angle versus load for (a, b) bearing A, (c, d) bearing B, (e, f) bearing C with different shafts under aligned condition.

but the bearing was used for some other tests before the test shown here and some scratches had left on the surface which can be seen in Figure 18Aa. These scratches have adverse effects on the lubrication performance of bearing. After the seizure test with shaft a, the surface became smoother and the effect of scratches was reduced. The effect of clearance on ε–F curve is not obvious for bearings B and C. This might be due to the measurement error.

The effect of journal surface roughness should be evaluated. In theory, the larger the longitudinal roughness, the larger the eccentricity ratio [9]. Here the surface roughness of shaft b (Ra0.31–0.35) is larger than that of shaft a (Ra0.09–0.12), but the eccentricity ratio is smaller

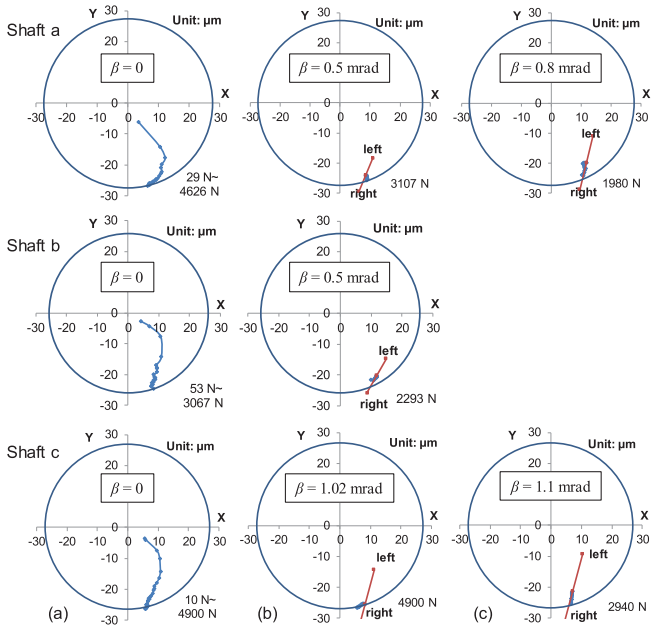

Fig. 14. Bearing A & different shafts: change of journal center position as (a) load increases and (b, c) misalignment angle increases. Blue line: locus of journal center on the mid-plane of bearing. Red line: projection of shaft axis on the mid-plane of bearing for seizure load under misaligned conditions.

for bearing A with shaft b. It indicates that the journal surface roughness has a smaller influence on eccentricity ratio than the radial clearance here.

The surface roughness of bearing B is the largest (Ra0.78–1.3 μm), followed by bearings C (Ra0.66–0.97 μm) and A (Ra0.31–0.36 μm). Compared with the surface roughness values of shafts, they are much larger. By comparing the ε–F curves of all tests except the test of bearing A with shaft a, it can be found that under a certain load, the eccentricity ratio of bearing A is the smallest, and that of bearing B is the largest. Thus, the larger the bearing surface roughness, the larger the eccentricity ratio. It indicates that the effect of bearing surface roughness (variation: about 1.3 μm) on eccentricity ratio is larger than that of radial clearance (variation: 1–1.5 μm), and is much larger than that of journal surface roughness (variation: 0.23 μm). Actually, the bearing lubrication performance is affected by the equivalent surface roughness, $R_{a,eq}$, which is equal to $\sqrt{{R_{a,j}}^2 + {R_{a,b}}^2}$. As the journal surface roughness is small, the bearing performance is mainly affected by the bearing surface roughness.

Figures 14–16 present change of journal center position as load increases and misalignment angle increases for different bearings and shafts. The shaft rotates counterclockwise. The circle is the clearance circle. The blue line is locus of journal center on the mid-plane of bearing as load increases and the red line is the projection of shaft axis on the mid-plane of bearing for seizure load under misaligned conditions. The left (right) point is the journal center on the left (right) plane of bearing. The load range and misalignment angle are shown in the figures.

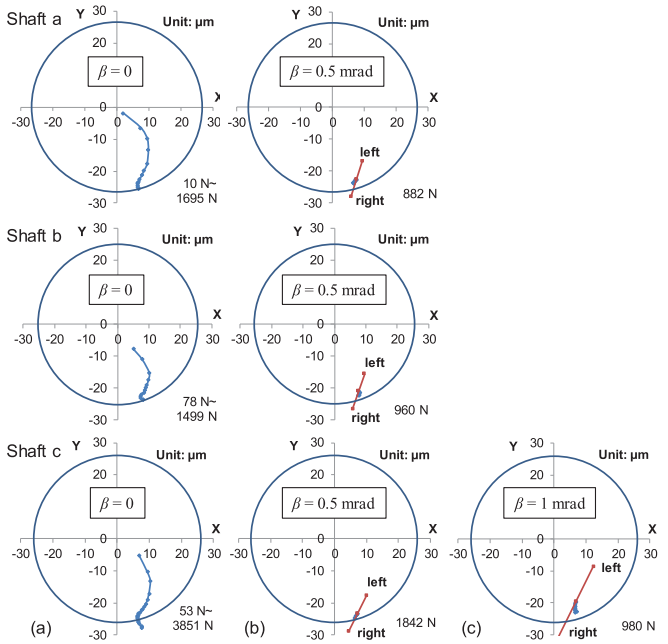

Fig. 15. Bearing B & different shafts: change of journal center position as (a) load increases and (b, c) misalignment angle increases.

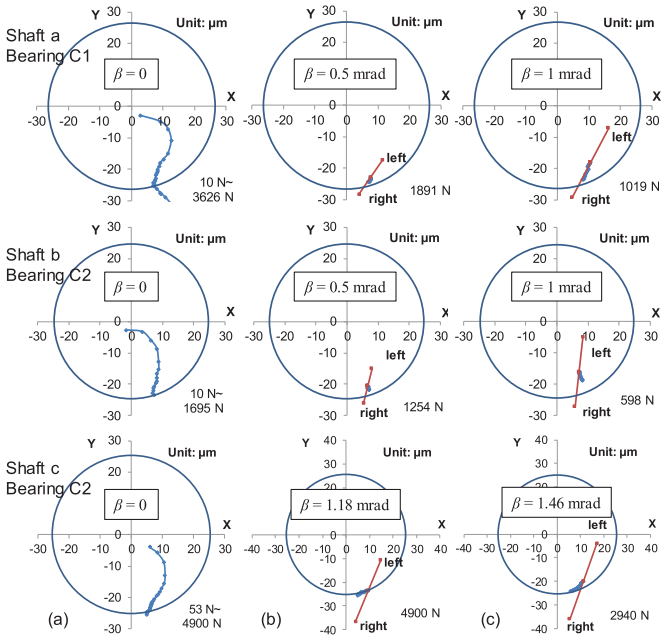

Fig. 16. Bearing C & different shafts: change of journal center position as (a) load increases and (b, c) misalignment angle increases.

Table 7. Journal center displacement, Δd_{jc}, and bearing deformation at the edge, t_{def}, of different friction pairs for misaligned conditions.

Shaft	a (Steel)				b (Steel)				c (DLC coating)			
Bearing	β/mrad	F_s/N	Δd_{jc}/μm	t_{def}/μm	β/mrad	F_s/N	Δd_{jc}/μm	t_{def}/μm	β/mrad	F_s/N	Δd_{jc}/μm	t_{def}/μm
A (Gray iron)	0.5	3107	1.7	2.7	0.5	2293	2.2	1.3	1.02	4900	2.6	10.1
	0.8	1980	4.5	2.8	–	–	–	–	1.1	2940	3.9	6.9
B (Aluminum1)	0.5	882	1.7	2.2	0.5	960	1.3	2.3	0.5	1842	1.7	3.3
	–	–	–	–	–	–	–	–	1	980	3.3	4.7
C (Aluminum2)	0.5	1891	1.5	2.2	0.5	1254	1.3	2.1	1.1	4900	4.8	11.4
	1	1019	6.0	3.1	1	598	3.0	3.2	1.46	2940	7.0	11

For a certain load, as the misalignment angle increased, at first the journal and the bearing contacted at the bottom right edge of the bearing, then it could be felt that the misalignment moment for increasing the misalignment angle increased immediately during the experiment. Subsequently, the journal center on the mid-plane of bearing moved upwards in the clearance circle as shown in Figures 14–16b, c. From the figures, it can also be seen that the right point lies outside of the clearance circle, which means that the bearing was deformed at the contact area under the vertical load and misalignment moment.

Table 7 summarizes the journal center displacement and bearing deformation at the edge of different friction pairs under misaligned conditions, and the results are drawn in Figure 17 for comparison. From Figure 17a it can be seen that under misaligned conditions, as the seizure inclined angle increases from 0.5 mrad to 1 mrad, the displacement of journal center increases for all conditions and the variations are 1.3–4.5 μm. It means that the journal center moves more easily for low load conditions. Figures 17b and d show that as the seizure inclined angle increases, the bearing deformation increases for all conditions except the tests of shaft c with bearings A and C. This is because the seizure load is lower for a larger inclined angle, thus there should be a larger deformation of bearing and larger contact area for the friction torque reaching the seizure torque. It can also be seen that the deformations at the edge of bearings A–C with shafts a and b are about 2 μm for $\beta = 0.5$ mrad, and about 3 μm for $\beta = 1$ mrad. For the tests of shaft c with bearings A and C, as the friction coefficient is very low, the seizure load is very high and the bearing deformation under misaligned conditions is

very large. The maximum bearing deformation is 10.1 μm for bearing A and 11.4 μm for bearing C. As the seizure inclined angle increases, their bearing deformation decreases. This can be explained by Figures 14b,c and 16b,c. When the seizure load is 4900 N, the eccentricity ratio changes very small as the inclined angle increases. While for $F_s = 2940$ N, it changes much larger. This causes the decrease of bearing deformation. Compared the results of different bearings, it can be found that the lower the friction coefficient of the friction pair, the larger the deformation at the edge when seizure happens.

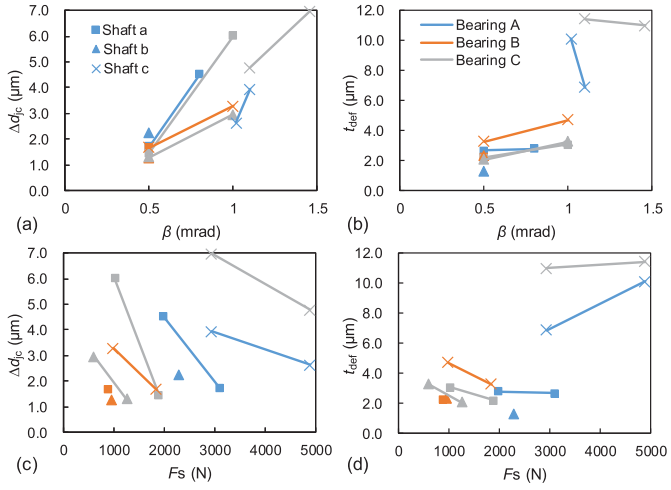

Fig. 17. The variation of journal center displacement, Δd_{jc}, and bearing deformation at the edge, t_{def}, with (a, b) inclined angle and (c, d) seizure load for different friction pairs under misaligned conditions.

4.3 Bearings and shafts after seizure tests

Figure 18 presents the bearing inner surfaces before and after experiments. The sequence of experiments is: shaft a, shaft b and shaft c. The polishing scratches can be seen clearly. After the seizure tests with shaft a, bearings A and B have only a few signs of wear because it was easy to tell when seizure happened and the running time was not long. For bearing C1, as it was difficult to determine the seizure load, the bearing ran for a long time (about 20 hours). The bearing was worn seriously under heavy load due to its poor wear resistance, as shown in Figure 18Ca. The diameter increased about 30 μm. Besides, the oil turned black as shown in Figure 19. This didn't happen in the experiments of other bearings. Bradshaw [27] undertook a full investigation on the causes of the phenomenon of "black oil". He found that the black oil formation had no relation to cleanliness or chemistry related issues, and it was mainly caused by the high concentrations of wear particles (3 to 5 μm). That is, excessive wear of bushing will make the oil turn black. It should be avoided in practical use. Bearing C2 was used for the seizure tests with shafts b and c, and to avoid wear the load at which the friction didn't decrease and began to increase was considered as its seizure load.

From the changes of bearing surfaces after seizure tests with shafts a, b and c, it can be seen that the signs of wear become more obvious as the running time under heavy load increases. The wear area becomes larger and the surface roughness in the wear area become smaller. After seizure tests with shaft c, the wear areas of bearings A, B and C are much larger than those after seizure tests with shafts a and b. This is because the seizure loads of bearings A, B and C with shaft c are much larger than those with shafts a and b

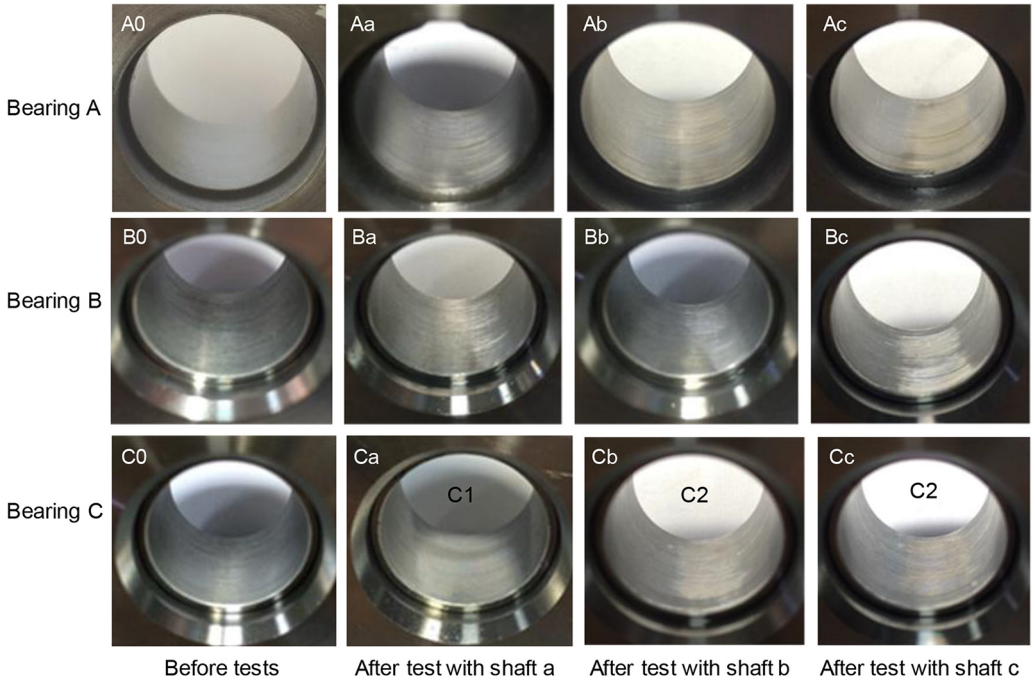

Fig. 18. Test bearings before and after experiments.

and the experimental time increases. According to the test procedure, the experimental time is proportional to seizure load. The more the experimental time, the larger the wear area.

Figure 20 shows the surfaces of three shafts after experiments. For shafts a and b, there is marks of running in, but the change of shaft diameter is very small. For shaft c, there are no major scratches. This indicates that the DLC coating has good wear resistance due to its high hardness.

4.4 Error analysis

Due to the imperfection of the test rig, the friction torque cannot be measured accurately by force sensor 2. The seizure load was estimated according to the variation of the measurement. The measuring method of friction torque and the determination method of seizure load cause the measurement error of seizure load. The error is about 50 N for low load conditions and 100 N − 200 N for high load conditions (more than 2000 N). To reduce the experimental error and study the variation of friction coefficient during the seizure test, the test rig could be improved by replacing the ball bearings with hydrostatic bearing.

The bearing diameter is small and thus the surface curvature influences the measurements. It is relatively difficult to determine the measurements when the x coordinate of the shaft center is zero. Thus, when analyzing the journal center position, the position shown in Figure 4a was considered as the standard position. The x coordinate of journal center, x_0, was determined approximately by the wear position on the bearing surface. But as the wear area is large especially for aluminum alloy bearings, the x coordinate of center of the wear area was used. Thus, there is error of x_0, and the error is about 3–4 μm. In other words, the actual position of the journal center locus in the clearance circle may be a little different from those shown in Figures 14–16, but the trajectory shape is the same. The error of x_0 mainly affects the attitude angle, and its influence on eccentricity is marginal.

The temperature was not studied in this work because it is difficult to deploy thermocouples without affecting the lubrication performance of the bearing. It will be studied in future work.

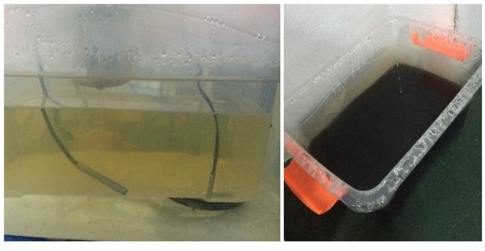

Fig. 19. Change of oil after the experiments of bearing C1 with shaft a.

5 Conclusions

In this paper, the seizure loads of journal bearings with three kinds of bushing materials under both aligned and misaligned conditions are investigated experimentally. The experimental results are summarized in Table 6. The effects of bushing material, shaft coating, and journal surface roughness on seizure load are discussed. The journal center locus is presented and the effects of radial clearance and surface roughness on ε–F curve are discussed. From the experimental results, the following conclusions are drawn:

- When the shaft material is 40Cr steel, the seizure load of Grade 250 gray iron is the highest, and the seizure load of the aluminum alloy with larger hardness is the lowest under both aligned and misaligned conditions.
- When there is a layer of DLC coating on the shaft surface, the seizure loads of the aluminum alloy with lower hardness and Grade 250 gray iron are the highest, and the seizure load of the aluminum alloy with larger hardness is the lowest. The DLC coating helps to improve the seizure load of these bearings under both aligned and misaligned conditions, as well as the maximum inclined angle under certain load.
- The bearing and journal surface roughness values have a considerable effect on seizure load of bearing, especially for aligned condition. The smaller the roughness, the larger the seizure load.
- The load carrying capacity of bearing is very low (< 400 N) for $\varepsilon < 0.7$ and increases sharply when $\varepsilon > 0.9$. The attitude angle decreases from about 60° to about 10° as the load increases.
- The surface roughness and radial clearance affect the ε–F curve. And the effect of bearing surface roughness (variation: about 1.3 μm) on ε is larger than that of radial clearance (variation: 1–1.5 μm), and is much larger than that of journal surface roughness (variation: 0.23 μm).
- For a certain load, as the misalignment angle increased, the journal center on the mid-plane of bearing moved upwards, and the bearing is deformed at the contact area.

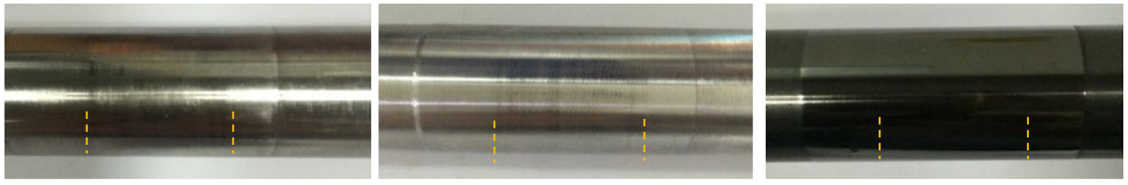

Fig. 20. Shafts after experiments.

The lower the friction coefficient of the friction pair, the larger the deformation at the edge when seizure happens.
– Excessive wear of bushing will make the oil turn black.

Nomenclature

a_i (b_i, c_i, d_i) (i =1, 2...)	Measurement of sensor a (b, c, d) for different conditions
Δa_i (Δb_i, Δc_i, Δd_i)	Measurement variation of sensor a (b, c, d) because of the shaft deformation under the same load as ai (bi, ci, di)
c	Radial clearance
d	Journal diameter
d_h	Diameter of oil hole
D	Bearing diameter
E	Elastic modulus
F	Load carrying capacity of journal bearing
F_s	Seizure load of journal bearing
L	Bearing length
L_1	Distance between sensor a (b) and sensor c (d)
N	Rotational speed of journal
p_s	Specific pressure, $=F/DL$
$R_\mathrm{a,b}$	Bearing surface roughness
$R_\mathrm{a,j}$	Journal surface roughness
$R_\mathrm{a,eq}$	Equivalent surface roughness
Δd_jc	Journal center displacement as load increases
t_def	Bearing deformation at the edge for seizure load under misaligned condition
x, y, z	Coordinates of the bearing system
β	Inclined angle
ε	Eccentricity ratio
ϕ	Attitude angle
ν	Poisson's ratio
μ	Oil viscosity
ρ	Oil density

The financial supports from National Natural Science Foundation of China (Grant No. 51905317) and Daikin Industries Ltd. are gratefully acknowledged.

References

[1] X. Zhang, Z. Yin, D. Jiang, G. Gao, Y. Wang, X. Wang, Load carrying capacity of misaligned hydrodynamic water-lubricated plain journal bearings with rigid bush materials, Tribol. Int. **99**, 1–13 (2016)
[2] X. Zhang, Z. Yin, Q. Dong, An experimental study of axial misalignment effect on seizure load of journal bearings, Tribol. Int. **131**, 476–487 (2019)
[3] B. S, R.P. K., Tribological properties of cast graphitic-aluminium composites, Tribol. Int. **16**, 89–102 (1983)
[4] T. Desaki, Y. Goto, S. Kamiya, Development of the aluminum alloy bearing with higher wear resistance, JSAE Rev. **21**, 321–325 (2000)
[5] E. Feyzullahoglu, N. Sakiroglu, The wear of aluminium-based journal bearing materials under lubrication, Mater. Des. (1980–2015) **31**, 2532–2539 (2010)
[6] B.K. Prasad, Sliding wear response of a grey cast iron: effects of some experimental parameters, Tribol. Int. **44**, 660–667 (2011)
[7] F. Summer, F. Grün, J. Schiffer, I. Gódor, I. Papadimitriou, Tribological study of crankshaft bearing systems: comparison of forged steel and cast iron counterparts under start-stop operation, Wear **338–339**, 232–241 (2015)
[8] S. Guha, Analysis of steady-state characteristics of misaligned hydrodynamic journal bearings with isotropic roughness effect, Tribol. Int. **33**, 1–12 (2000)
[9] N.M. Bujurke, N.B. Naduvinamani, S.T. Fathima, S.S. Benchalli, Effect of surface roughness on couple stress squeeze film lubrication of long porous partial journal bearings, Ind. Lubric. Tribol. **58**, 176–186 (2006)
[10] J. Sun, X. Zhu, L. Zhang, X. Wang, C. Wang, H. Wang, X. Zhao, Effect of surface roughness, viscosity-pressure relationship and elastic deformation on lubrication performance of misaligned journal bearings, Ind. Lubric. Tribol. **66**, 337–345 (2014)
[11] J. Bouyer, M. Fillon, An experimental analysis of misalignment effects on hydrodynamic plain journal bearing performances, J. Tribol. **124**, 313–319 (2002)
[12] I. Pierre, J. Bouyer, M. Fillon, Thermohydrodynamic behavior of misaligned plain journal bearings: theoretical and experimental approaches, Tribol. Trans. **47**, 594–604 (2004)
[13] J. Sun, C. Gui, Z. Li, An experimental study of journal bearing lubrication effected by journal misalignment as a result of shaft deformation under load, J. Tribol. **127**, 813–819 (2005)
[14] J. Sun, C.L. Gui, Z.Y. Li, Z. Li, Influence of journal misalignment caused by shaft deformation under rotational load on performance of journal bearing, Proc. Inst. Mech. Eng. J **219**, 275–283 (2005)
[15] P.G. Nikolakopoulos, C.A. Papadopoulos, A study of friction in worn misaligned journal bearings under severe hydrodynamic lubrication, Tribol. Int. **41**, 461–472 (2008)
[16] P. Nikolakopoulos, C. Papadopoulos, Wear model evaluation in misaligned journal bearings, in Proceedings of the 3rd International Conference on Power transmissions, 2009.
[17] K. Thomsen, P. Klit, Improvement of journal bearing operation at heavy misalignment using bearing flexibility and compliant liners, Proc. Inst. Mech. Eng. J **226**, 651–660 (2012)
[18] R. Mallya, S.B. Shenoy, R. Pai, Steady state characteristics of misaligned multiple axial groove water-lubricated journal bearing, Proc. Inst. Mech. Eng. J **229**, 712–722 (2014)
[19] R. Mallya, S.B. Shenoy, R. Pai, Static characteristics of misaligned multiple axial groove water-lubricated bearing in the turbulent regime, Proc. Inst. Mech. Eng. J **231**, 385–398 (2016)
[20] J. Li, H. Cao, L. Lv, H. Yang, L. Zhang, Influence of dissimilar radial clearances on the performance of hydrodynamic rotor-bearing systems considering misalignment effects, Proc. Inst. Mech. Eng. J **232**, 231–243 (2017)

[21] F. Lv, N. Ta, Z. Rao, Analysis of equivalent supporting point location and carrying capacity of misaligned journal bearing, Tribol. Int. **116**, 26–38 (2017)
[22] B. Li, J. Sun, S. Zhu, Y. Fu, X. Zhao, H. Wang, Q. Teng, Y. Ren, Y. Li, G. Zhu, Effect of the axial movement of misaligned journal on the performance of hydrodynamic lubrication journal bearing with rough surface, Mech. Ind. **20**, 402 (2019)
[23] Y. Zhang, G. Chen, L. Wang, Thermoelastohydrodynamic analysis of misaligned bearings with texture on journal surface under high-speed and heavy-load conditions, Chin. J. Aeronaut. **32**, 1331–1342 (2019)
[24] J. Mo, Y. Luo, J. Liu, D. Yan, X. Chen, C. Li, C. Duan, Z. Zhu, Y. Shen, H. Du, Experimental and numerical study of the pre-tilted journal bearing, Proc. Inst. Mech. Eng. J **2019**, 135065011989519 (2019)
[25] L. Zheng, H. Zhu, J. Zhu, Y. Deng, Effects of oil film thickness and viscosity on the performance of misaligned journal bearings with couple stress lubricants, Tribol. Int. **146**, 106229 (2020)
[26] S. Zhu, J. Sun, B. Li, G. Zhu, Thermal turbulent lubrication analysis of rough surface journal bearing with journal misalignment, Tribol. Int. **144**, 106109 (2020)
[27] S. Bradshaw, Investigations into the contamination of lubricating oil in rolling element pump bearing assemblies, in Proceedings of the 17th International Pump Users Symposium, Texas A&M University. Turbomachinery Laboratories, 2000.

Cite this article as: X. Zhang, Z. Yin, Q. Dong, J. Cao, Experimental comparison of the seizure loads of gray iron journal bearing and aluminum alloy journal bearing under aligned and misaligned conditions, Mechanics & Industry **21**, 408 (2020)